SLAC – PUB – 3754
August 1985
(E)

RECENT RESULTS OF THE STUDY OF PHOTON–PHOTON COLLISIONS*

J. C. SENS†

Stanford Linear Accelerator Center
Stanford University, Stanford, California, 94305

ABSTRACT

Results are reported on the production of two– and four–hadron final states, and on the formation of the η, η' and f mesons in photon–photon collisions.

Invited paper presented at the Physics in Collision V Conference,
Autun, France, July 3–5, 1985.

* Work supported in part by the Department of Energy, contract DE-AC03-76SF00515, by the National Science Foundation, by the Joint Japan-United States Collaboration in High Energy Physics and by the Foundation for Fundamental Research on Matter in the Netherlands.

† Permanent address: National Institute for Nuclear and High Energy Physics, Amsterdam, the Netherlands.

1. INTRODUCTION

1.1 TOPICS TO BE DISCUSSED

When photons are made to collide with photons they interact by virtue of the fact that, due to quantum fluctuations of the vacuum, the $\gamma\gamma$ initial state:

$$|\Psi\rangle = a|\gamma,\gamma\rangle + b|\gamma,l\bar{l}\rangle + c|\gamma,q\bar{q}\rangle + d|l\bar{l},l\bar{l}\rangle + \cdots . \qquad (1.1)$$

contains, in addition to a "classical", non-interacting term (representing the superposition of two electromagnetic waves), "quantum" terms which give rise to observable final state particles. The situation is analogous to that of the electron/muon g-factor: $g = 2 + (\frac{\alpha}{\pi} + c\frac{\alpha^2}{\pi^2} + \cdots)$, which differs from the classical value (g=2) only by virtue of quantum effects. In addition to the terms in (1.1) there are terms containing bound states of quarks of finite spatial extent ($|\gamma,\rho\rangle, |\gamma,\phi\rangle, |\rho,\rho\rangle$, etc.) which dominate the $\gamma\gamma$ interaction at low momentum transfer. The $\gamma\gamma$ interaction cross section, of order 10^{-70} cm^2 for photons in the range of visible light[1] and too small also to contribute to the lepton pair production by cosmic ray photons interacting with temperature radiation of interstellar matter[2] increases with energy as ln s and gives rise to managable event rates at current (PETRA, PEP) and future (SLC, TRISTAN, LEP) collidor energies.

In the following, results obtained since mid-1984 will be reported on two topics: the production of two- and four- hadron final states, ($\pi\pi$, KK, $\pi\pi\pi\pi$, $\pi\pi$ KK, $\pi\pi p\bar{p}$) , and the formation and decay of $\eta \to \gamma\gamma$, $\eta' \to \pi\pi\gamma$ and f $\to \pi\pi$. Earlier results, not detailed here, are:

- The leptonic structure function of the photon in $ee \to ee\mu\mu$; good agreement is found with QED to order α^4.
- The $\gamma\gamma$ total cross section for the production of hadrons; $\sigma(\gamma\gamma \to X) \approx$ 300 nb at $Q^2 = 0$, flat in $2 < W_{\gamma\gamma} < 20$ GeV, with a Q^2 dependence indicative of Vector Meson Dominance.

– The hadronic structure function of the photon; in both its x ($= Q^2/(Q^2 + W^2_{\gamma\gamma})$) and Q^2 dependence point–coupling effects of photons to quarks ((1.1)) are discernable and become more pronounced in subsets of two–jet final states with high p_T^{JET} and high Q^2.

1.2 SELECTION OF EVENTS

Most of the data to be discussed have been obtained with the PEP4/9 detector at PEP. Its major components are : the TPC, four calorimeters, and a nearly 4π muon detector. The data have been selected with a variety of triggers and off–line filters:

– $\geq$ 2 charged tracks in the TPC, "inner" and "outer" drift chamber hits within a suitable fiducial volume, and a vertex near the collision point. Tags are not required in this trigger. Off–line filters include a total energy $<$ 12 GeV (to reject annihilation events), a balanced overall p_T (to ensure exclusive final states), and lower thresholds on polar angles and p_T of the tracks (to avoid regions of rapidly varying acceptance and to reject QED–induced background). Two– and four– prong events, $\eta' \rightarrow \pi\pi\gamma$ events at $Q^2 = 0$, and f $\rightarrow \pi\pi$ events were selected in this way.

– Minimum energy deposition in the forward calorimeters (to trigger on tags), and $\geq$ 1 charged track centrally (to reject QED background), along with zero net charge, a balanced p_T and lower limits on θ, p_T per track (to ensure exclusivity) in the off–line filter. Two– and four–prong events at $Q^2 > 0$ were selected in this way.

– An all–neutral trigger for the selection of $\gamma\gamma \rightarrow \eta \rightarrow \gamma\gamma$ events, requiring two localized showers in one of two 14 X_o deep, MWPC/Pb–laminate calorimeters (PTC) covering $16° < \theta < 32°$. Off–line filters include vetoes on charged prongs, on additional showers, and the presence of tracks in the path connecting the PTC showers to the collision point.

1.3 PARTICLE IDENTIFICATION

Particles are identified by means of requirements on dE/dx, depth of penetration into the muon detectors, and the momentum/energy ratio of electrons detected in the TPC and the calorimeters. The effectiveness of this selection is limited by cross–overs in the dE/dx versus p curves for different particle types in the range of momenta of interest in 2γ events, the lack of distinction between dE/dx for pions and muons, a $\sim$ 1.0 GeV/c cutoff in the muon detector, and the limited efficiency of the tracking devices, in particular those in the forward direction.

For each track detected in the TPC, a number of dE/dx samples (min 30, max 183) is required from which a truncated mean, using the lowest 65% of the samples, is calculated. A χ^2 fit is then made to a theoretical dE/dx versus momentum curve, calculated for each particle type. By convention, a particle is *unambiguously* identified, if its $\chi^2 + 4$ is less than the χ^2 for any other particle type, and is considered to be *consistent* with a e, π/μ, K or p hypothesis if its $\chi^2 < 8$ .Some additional dE/dx requirements have been imposed in the selection of specific final states .

2. PRODUCTION OF TWO– AND FOUR–PRONG HADRONIC FINAL STATE

2.1 THE PRODUCTION OF PAIRS OF PSEUDOSCALAR MESONS

Brodsky and Lepage[8] have pointed out long ago that 2 body–production processes $\gamma\gamma \to h\bar{h}$ at large $W^2_{\gamma\gamma}$, are characterized by an amplitude of the form:

$$M(W_{\gamma\gamma}, \theta_{CM}) = \int \phi^*_h(x_i)\, \phi_{\bar{h}}(x'_j)\, \mathrm{T}(x_i, x'_j, W_{\gamma\gamma}, \theta_{CM}) \qquad (2.1)$$

where $\phi(x)$ is the parton distribution function in the hadron and T the amplitude for scattering parton i in h off parton j in $\bar{h}$ (sums over final states, Q^2, helicities

have been omitted), and obey a scaling law at fixed θ_{CM}:

$$\frac{d\sigma}{d\cos\theta_{CM}}(\gamma\gamma \to \pi\pi) = c\,\frac{\alpha^2\alpha_s^2}{W_{\gamma\gamma}^6}\,\frac{1}{\sin^4\theta_{CM}} \tag{2.2}$$

with a known absolute normalization constant c, which is proportional to the $\pi \to \mu$ decay constant f_π. Furthermore,

$$d\sigma(\gamma\gamma \to \mathrm{KK}) = \left(\frac{f_\mathrm{K}}{f_\pi}\right)^4 d\sigma(\gamma\gamma \to \pi\pi) \tag{2.3}$$

Experimentally, the major problem is the unambiguous identification of a small number of $\pi\pi$ pairs in a sea of $\mu\mu$ pairs which nearly identical dE/dx:

$$\frac{ee \to ee\pi\pi}{ee \to ee\mu\mu} << 1 \text{ and } \left(\frac{dE}{dx}\right)_\mu \approx \left(\frac{dE}{dx}\right)_\pi \tag{2.4}$$

The π/μ ambiguity can be resolved by means of a statistical procedure[4] which employs, per mass bin, the difference in χ^2 for the pion and muon hypothesis to extract the fractions. At $\pi\pi$ masses $\gtrsim$ 1.0 GeV, the χ^2s become indistinguishable and, instead, the μ pairs are required to penetrate the iron of the muon chambers. The (one-hit) muon detector efficiency is > 90% for $p_T \gtrsim$ 1 GeV/c. Decay and punch-through corrections amount to 2% and 10% respectively. The $\pi\pi$ cross section is then obtained from the fractions and the QED cross section for the process $\gamma\gamma \to \mu\mu$.

Fig.2.1 a shows the $\pi\pi$ cross section and its $W_{\gamma\gamma}$ dependence in comparison with the Brodsky/Lepage calculations. For $W_{\gamma\gamma} \lesssim$ 1.5 GeV, the f(1270) dominates the cross section. For $W_{\gamma\gamma} \gtrsim$ 2.0 GeV, the $W_{\gamma\gamma}$ dependence is in fair agreement with (2.1) . For 1.5 < $W_{\gamma\gamma}$ < 2 GeV, the data are a factor of 3–4 above the calculated σ, possibly as a result of resonance/continuum interference. Fig. 2.1 b shows MARK II (at PEP) results[5] on $\pi\pi$ + KK; they exhibit a similar trend.

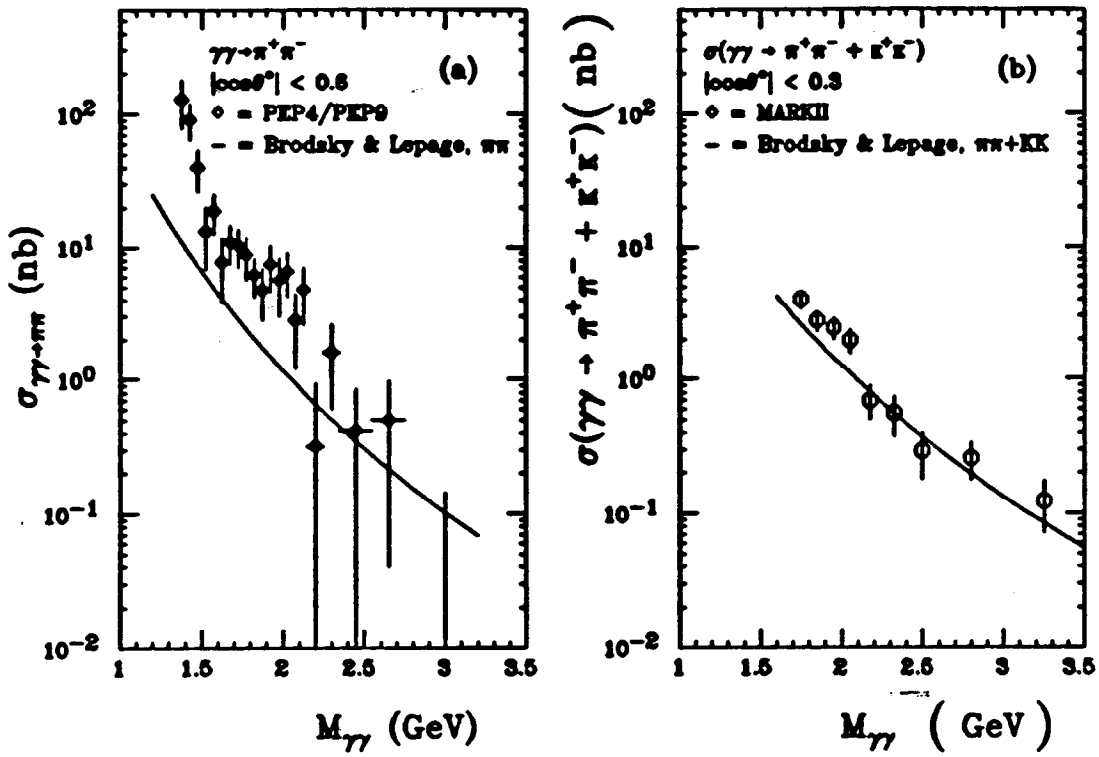

Fig. 2.1 *The $\pi\pi$ continuum data of PEP4/9 (a) and MARKII (b), compared to the QCD calculation of Brodsky and Lepage*[8]

The KK data are shown in Fig.2.2 . There is excellent agreement both in $W_{\gamma\gamma}$ dependence and absolute normalization with (2.2) ,scaled by means of (2.3) . In both the $\pi\pi$ and KK data the angular range is confined to $|\cos\theta^*| < 0.6$, too limited for a check of the angular dependence in (2.2) .

In conclusion, the $\gamma\gamma \rightarrow$ KK data are in good agreement with the scaling law of (2.2) , which follows from the hard scattering amplitude T in (2.1) , calculated in leading order from QCD Born diagrams, neglecting quark and hadron masses. The lack of agreement for the $\gamma\gamma \rightarrow \pi\pi$ data at low mass can possibly be ascribed to interference of the continuum with the f(1270) and other resonances, completely or incompletely reconstructed as $\pi\pi$ final states . The results are insensitive to the particular form of the parton distribution amplitudes $\phi(x)$.

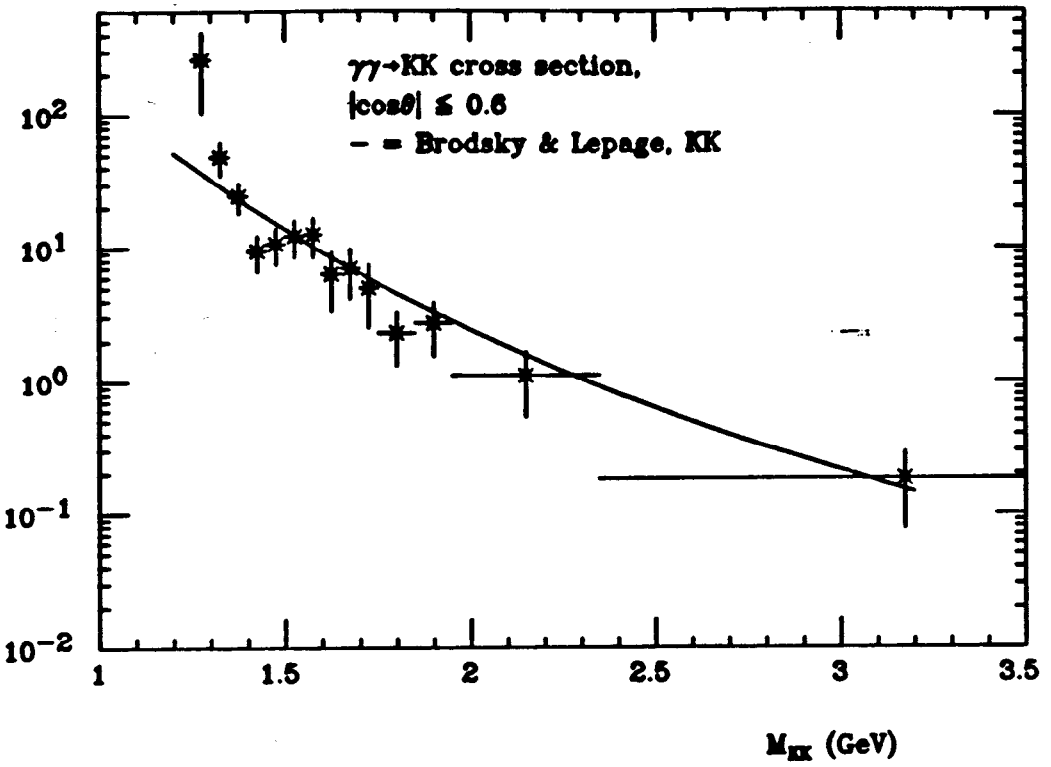

Fig. 2.2 *The KK continuum data of PEP4/9 (preliminary) , compared to the QCD calculation of Brodsky and Lepage*[8]

2.2 THE PRODUCTION OF PAIRS OF VECTOR MESONS

In the $\gamma\gamma \to \pi^+\pi^-\pi^+\pi^-$ mass spectrum there is a well-known enhancement over the QCD-predicted rate in the range $1.5 < W_{\gamma\gamma} < 2.5$ GeV. The main component, $\gamma\gamma \to \rho^0\rho^0$, exceeds 100 nb at $W_{\gamma\gamma} \approx 1.5$ GeV. The process $\gamma\gamma \to \rho^+\rho^-$ shows no such enhancement. These features can not be explained by means of a single resonance (which would require $\sigma(\rho^+\rho^-) = 2\sigma(\rho^0\rho^0)$ or $\sigma(\rho^+\rho^-) = \frac{1}{2}\sigma(\rho^0\rho^0)$ for an I=0 or I=2 resonance, respectively), but are compatible with two interfering four-quark states (a term $|q\bar{q},q\bar{q}\rangle$ in (1.1)). Fig.2.3 shows the available data and the 4-q model of Achasov et al[6] . If this model is correct, then $\sigma(\gamma\gamma \to \phi\rho^0)$ should be in the range 10–70 nb and $\sigma(\gamma\gamma \to K^*(890)\bar{K}^*(890))$ in the range 0.1–1.5 nb[7] .

Experimentally, final states with 4 charged prongs are relatively easy to iden-

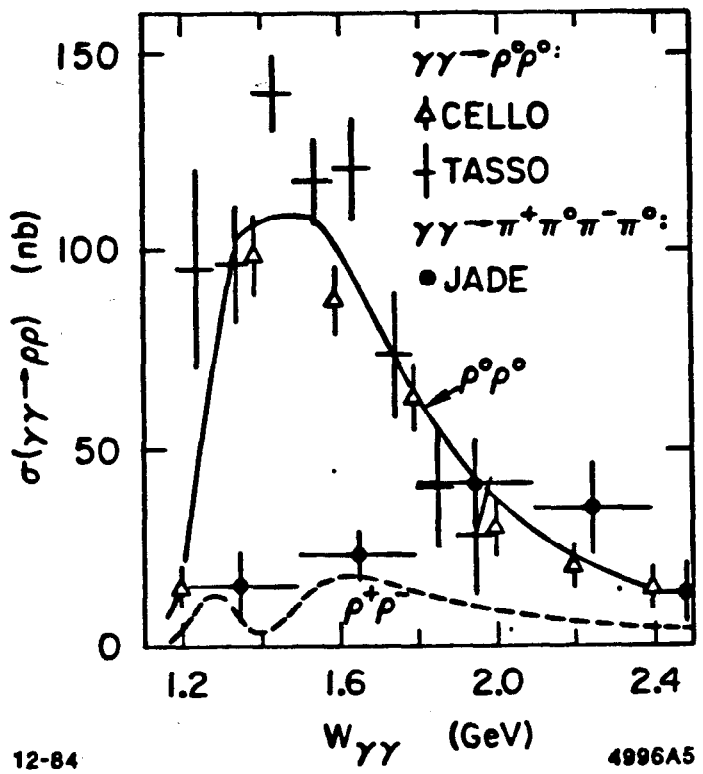

Fig. 2.3 *Data on $\rho^0\rho^0$ and $\rho^+\rho^-$ production , compared to the 4-quark model of Achasov et al*[16]

tify, since no calorimeters are involved (except in vetoing extra photons) and the muon background is absent. Fig. 2.4 shows the KK , $\pi\pi$ and $K\pi$ mass spectra for exclusive $\pi\pi$KK events. Both the tagged and untagged KK samples contain ϕ–mesons; they are not accompanied, however, by ρ's, as shown in Fig.2.4 c (shaded area). The upper limit is in accord with the 4–quark models:

$$\text{PEP4/9}: \quad \sigma(\gamma\gamma \to \phi\rho^0) < 2.7\,\text{nb (95\% CL)} \quad 2 < W_{\gamma\gamma} < 2.6\,\text{GeV}$$

$$\text{4q MODELS}: \quad = 2 - 16\,\text{nb} \quad 2 < W_{\gamma\gamma} < 2.6\,\text{GeV}$$

The unlike–sign Kπ mass plot (see Fig.2.4 d) of the same data set shows evidence for $K^{*0}(890)K\pi$ but no clear $K^{*0}\bar{K}^{*0}$ signal has been found. The upper limit is:

$$\text{PEP4/9}: \quad \sigma(\gamma\gamma \to K^{*0}\bar{K}^{*0}) < 5.7\,\text{nb (95\% CL)}$$

$$\text{4q MODELS}: \quad = 0.1 - 1.5\,\text{nb}$$

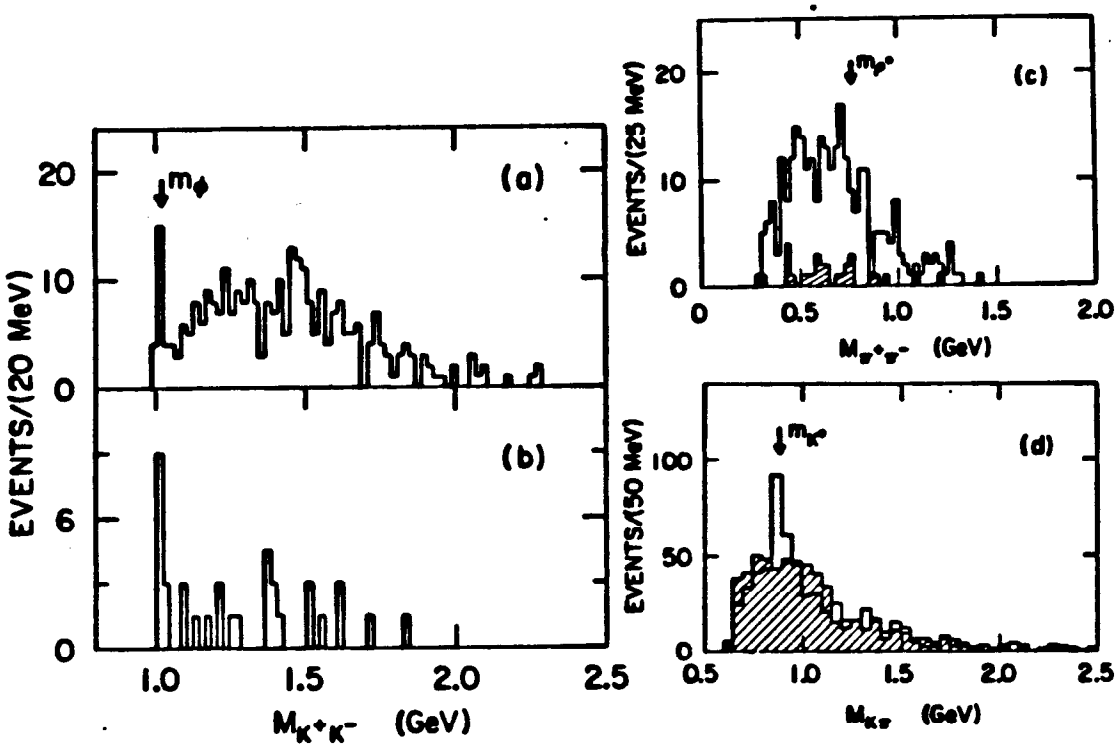

mass spectrum for untagged triggers;b.same for tagged triggers;c.$\pi\pi$ mass spectrum without and with (shaded) KK in the ϕ mass band d.unlike- and like-sign (shaded) $K\pi$ pairs , showing evidence for K^* production .

In contrast to the small cross sections for the production of vector meson pairs, there is a relatively large (not predicted) cross section for the production of the three body final states $\phi\pi\pi$ and $K^{*0}K\pi$, and the $KK\pi\pi$ continuum. The latter goes through a maximum of $\sim$ 15 nb in the range $2 < W_{\gamma\gamma} < 3$ GeV.

2.3 THE PRODUCTION OF PAIRS OF BARYONS

The production of pairs of baryons ($p\bar{p}, \Delta\bar{\Delta}, \Lambda\bar{\Lambda}$, etc.) is governed by a QCD–derived scaling law similar to the one of (2.2) :

$$\frac{d\sigma}{d\cos\theta}\ (\gamma\gamma \to B\bar{B}) \quad \sim \quad \frac{\alpha_s^4}{W_{\gamma\gamma}^{10}} f(\theta_{CM}) \qquad (2.5)$$

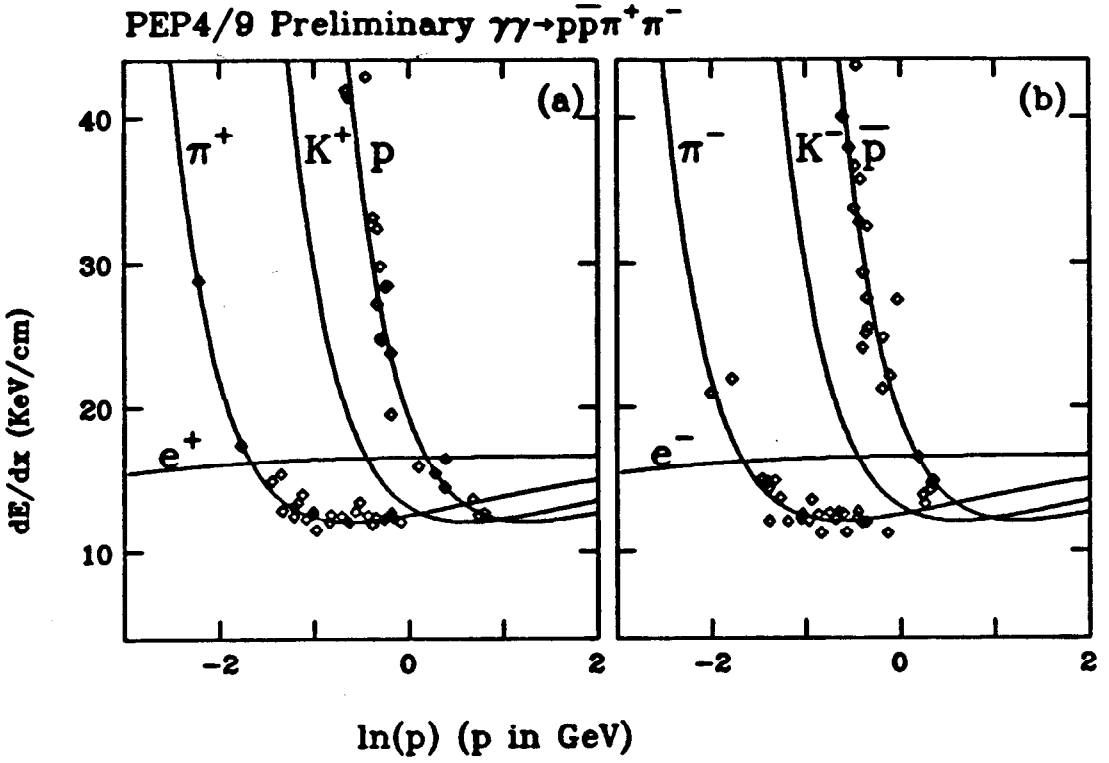

Fig. 2.5 *dE/dX distribution for exclusive $\pi^+\pi^-p\bar{p}$ events .*

Data on $\gamma\gamma \to p\bar{p}$ by the TASSO[6] collaboration agree with the $W_{\gamma\gamma}$ dependence of (2.5) ,but are a factor ~ 5 above the calculated[9] rate in the range $2.4 < W_{\gamma\gamma} < 2.8$ GeV. An earlier calculation[10] disagrees by a factor ~ 10. TASSO[11] has also searched $\pi^+\pi^-p\bar{p}$ final states for $\Delta^{++}\bar{\Delta}^{--}, \Delta^0\bar{\Delta}^0$ and $\Lambda\bar{\Lambda}$ final states and obtained upper limits, well above the calculated rates.

New data on $\gamma\gamma \to \pi^+\pi^-p\bar{p}$ have recently been obtained by the PEP4/9 collaboration. Particles were identified as described in section 1.3. The dE/dx of each of the particles in 27 events, in a 73pb^{-1} sample, surviving a $\sum p_T$ cut and a visual scan, is shown in Fig.2.5 . Pions and (anti) protons are clearly separated. Beam/gas background ($e^-p \to e^-p\pi^+\pi^-$) would result in a p/$\bar{p}$ asymmetry, in a concentration of events near the e/p crossover, a spread-out vertex distribution and a $\sum p_z \neq 0$, all contrary to observation. The cross section is shown in Fig. 2.6 , along with the TASSO data on $\gamma\gamma \to p\bar{p}$. The $\pi^+\pi^-p\bar{p}$ data are a factor ~ 10

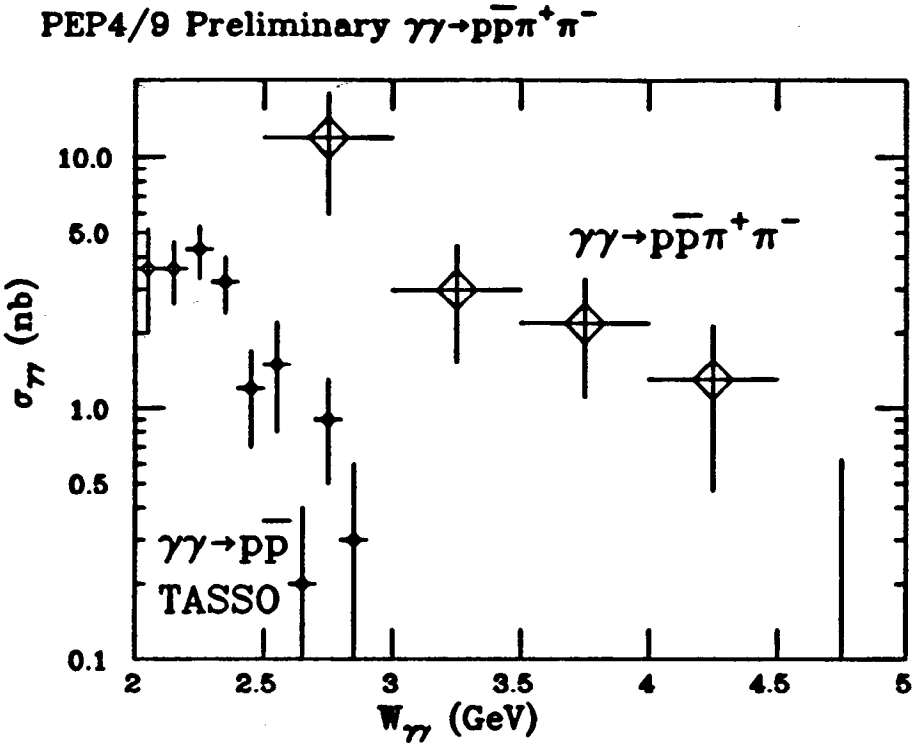

Fig. 2.6 *The cross section for exclusive* $p\bar{p}$ *(TASSO) and* $\pi\pi p\bar{p}$ *(PEP4/9) events*

above the $p\bar{p}$ data and follow a $W_{\gamma\gamma}^{-5.4\pm1.1}$ dependence. Of the 27 events none are compatible with $\Lambda\bar{\Lambda}$, 7 are compatible with $\Delta^0\bar{\Delta}^0$, 12 with $\Delta^{++}\bar{\Delta}^{--}$. The fact that 2/3 of the sample have both pion/(anti) proton combinations in the event near the Δ mass is compatible with phase space, since the threshold for $\pi^+\pi^-p\bar{p}$ production, and the $W_{\gamma\gamma}$ dependence of the $\gamma\gamma$ luminosity and the acceptance, all conspire to produce an accumulation of events in this region of phase space. The data are therefore not necessarily in contradiction with a $\Delta^{++}\bar{\Delta}^{--}$ production cross section $\sim W_{\gamma\gamma}^{-10}$ with $\sigma = 0.5$ nb at $W_{\gamma\gamma} = 2.4$ GeV, as expected[9] on the basis of (2.5) .

Another indication that most of the $\pi^+\pi^-p\bar{p}$ yield is not $\Delta\Delta$ is seen in the $\cos\theta^*$ distribution , where θ^* is the angle between the $p\pi$ pair and the $\gamma\gamma$ axis, and in the $\cos\theta_p$ distribution, where θ_p is the Δ decay angle in its c.m. frame with respect to the photon – photon axis. For a 2-body final state the $\cos\theta^*$

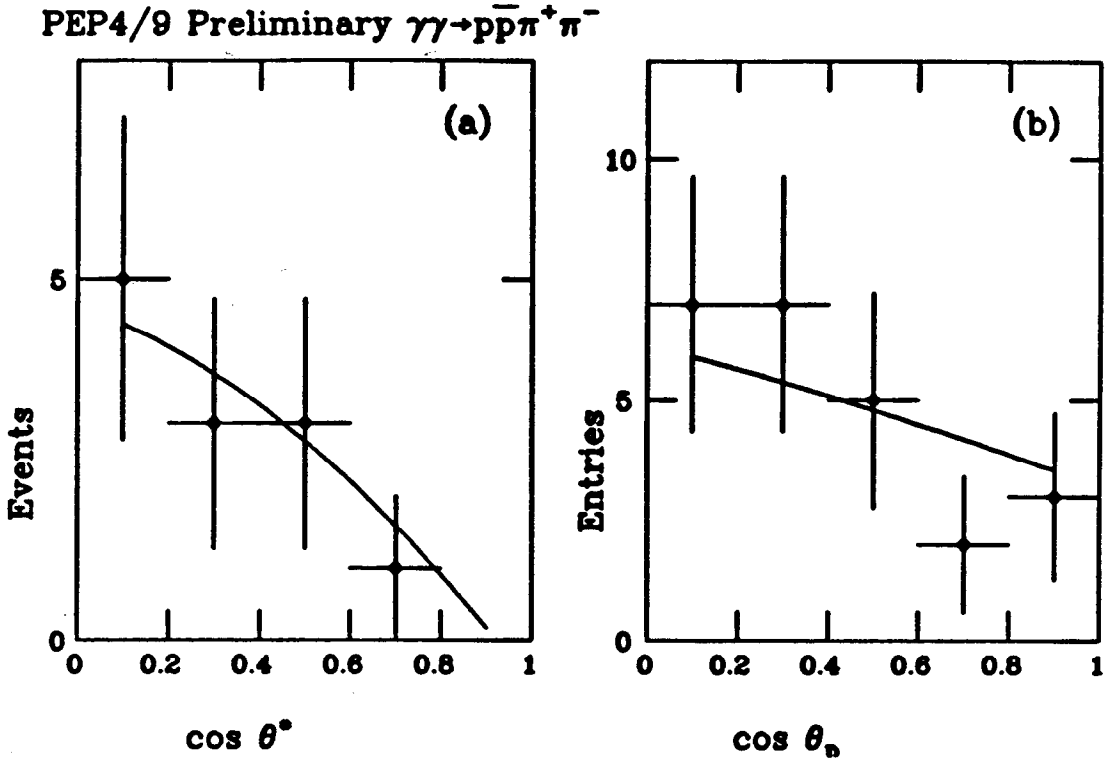

Fig. 2.7 *Angular distribution of events compatible with* $\gamma\gamma \to \Delta^{++}\bar{\Delta}^{--}$ *: (a)* θ^* *= angle of* pπ *with respect to the* $\gamma\gamma$ *axis ; (b)* θ_p *=decay angle of the delta in its c.m.,with respect to the direction of the photons.The solid lines correspond to phase space for accepted events.*

distribution is expected to have a steep angular dependence; both distributions are in agreement with the solid lines in Fig.2.7 ,which represent the angular distributions of isotropically – generated events, accepted by the detector.

One may speculate that a large fraction of the $\gamma\gamma \to p\bar{p}$ and the $\gamma\gamma \to \pi^+\pi^- p\bar{p}$ yield is the result of resonance formation ($\gamma\gamma \to X \to p\bar{p}$, $\gamma\gamma \to X \to \Delta\Delta$), not accounted for in the QCD Born diagrams from which the amplitude T in (2.1) is computed. This would qualitatively account for the prolific production of baryons and for the isotropy in the angular distribution. A search for structure in the $\pi^+\pi^-$ mass and $p\bar{p}$ mass distributions of the $\pi^+\pi^- p\bar{p}$ data had a negative result, making it unlikely that $\gamma\gamma \to p\bar{p}$ proceeds predominantly via resonance formation.

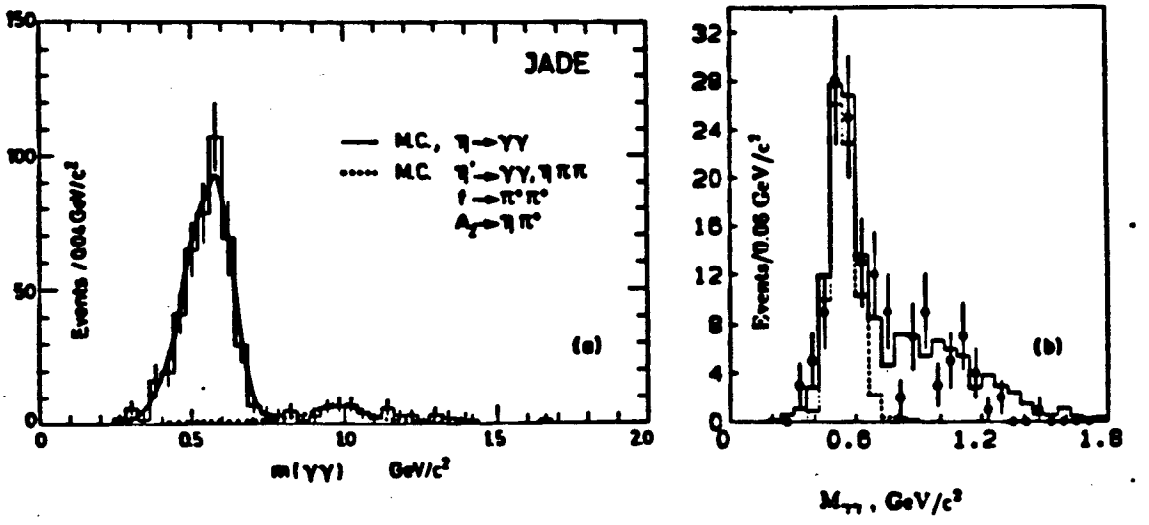

Fig. 3.8 *Mass distributions of $\gamma\gamma \rightarrow \eta \rightarrow \gamma\gamma$ events recorded in the JADE (a) and the PEP4/9 (b) detectors.*

In summary, it appears that the QCD calculations of baryon pair production underestimate the $\gamma\gamma \rightarrow p\bar{p}$ yield observed, and that, in $\pi^+\pi^- p\bar{p}$ final states, the normalization, the $W_{\gamma\gamma}$ dependence, and the angular distribution are in disagreement with predictions based on double - baryon production as the dominant contributor to the $\pi\pi p\bar{p}$ final state .

3. RESONANCE FORMATION IN $\gamma\gamma$ COLLISIONS

3.1 NEW DATA ON THE RADIATIVE WIDTH OF THE η, η', AND f MESONS

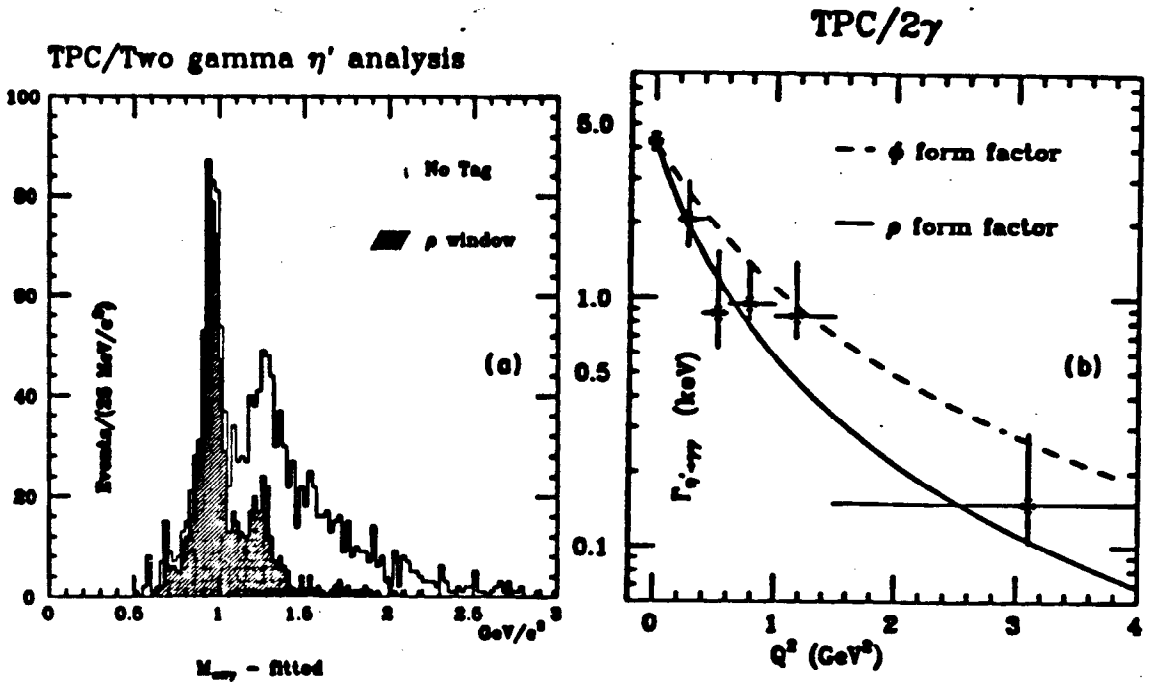

Fig. 3.9 *(a) mass and (b) Q^2 distribution of the η' (PEP4/9)*

JADE[12] and PEP4/9 have recently completed the analysis of $\gamma\gamma \to \eta \to \gamma\gamma$ events and determined the radiative width. Some characteristic features of the two experiments are shown in table 3.1 . The JADE trigger requires photons in the Pb-glass barrel, the PEP4/9 trigger requires forward photons in the end – cap Calorimeter. The overall detection efficiency of JADE is a factor of fifteen larger than that of PEP4/9. The Σp_T^2 and $\Delta\phi$ distributions indicate that the JADE detector is considerably more accurate than PEP4/9 in determining shower angles and energies. The η mass plots are shown in Fig. 3.8 .The results are :

$$\text{JADE} \quad \Gamma_{\eta\to\gamma\gamma} = 0.53 \pm 0.04 \pm 0.04\,\text{keV}$$

$$\text{PEP4/9} \quad \Gamma_{\eta\to\gamma\gamma} = 0.61 \pm 0.13 \pm 0.12\,\text{keV}$$

In PEP4/9 $\gamma\gamma \to \eta' \to \pi^+\pi^-\gamma$ events were identified in untagged and tagged charged particle triggers (section 1.2) and off-line-selected photons in the barrel

MEASUREMENTS OF $\Gamma_{\eta\to\gamma\gamma}$		
	PEP4/9	**JADE**
INT. LUMINOSITY pb^{-1}	67.5	31.7
MAIN TRIGGER REQUIREMENT	TWO LOCALIZED SHOWERS	2 OR 3 AZIM. Pb GLASS SEPTANTS
KINEMATIC SELECTION	$16° < \theta_\gamma < 32°$ $\Delta\phi < 45°$ $E_{\gamma\gamma} > 1.2$GeV	$47° < \theta_\gamma < 133°$ $\Delta\phi < 20°$ $E_\gamma > 140$MeV
HALFMAX. $\sum p_T^2$ (GeV^2)	~ 0.02	~ 0.003
HALFMAX. $\Delta\phi$	$\sim 10°$	$1°$
DETECTION EFF.	$\sim 0.17\%$	$\sim 2.5\%$
# EVENTS	70	442
$\sigma(ee\to ee\eta)\,(nb)$	1.55 ± 0.33	1.43 ± 0.11
$\Gamma_{\eta\to\gamma\gamma}$ (keV)	$0.61 \pm 0.13 \pm 0.12$	$0.53 \pm 0.04 \pm 0.04$

Table 3.1 *Features of the JADE and PEP4/9 measurements of the radiative width of the η .*

and end-cap calorimeters.The mass spectrum of the untagged events and the Q^2 dependence of tagged and untagged events is shown in Fig. 3.9 .Nearly all events are compatible with $\eta' \to \rho\gamma$. After subtraction of the background (mainly due to A_2 decay , with one photon undetected) 320 events remain in 74 pb^{-1} , with a (preliminary) radiative width at $Q^2 = 0$:

$$\Gamma_{\eta'\to\gamma\gamma} = 4.2 \pm 0.3 \pm 0.6\text{keV}$$

For $0 < Q^2 < 1$ the data agree with an earlier measurement[18] . For comparison, the Q^2 dependence of the ρ and ϕ form factors are also indicated in Fig. 3.9 .

The exclusive $\pi\pi$ final state, discussed in section 2.1 contains, in addition to the $\pi\pi$ continuum, a strong f(1270) signal, see Fig. 3.10 . Using the same

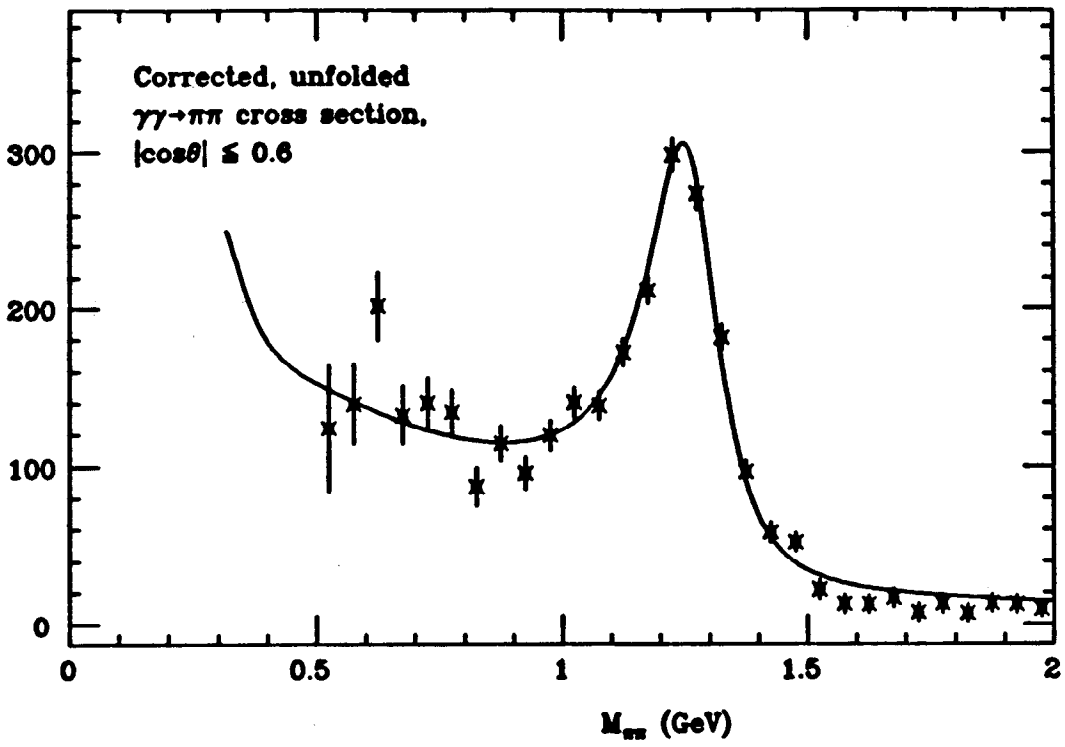

Fig. 3.10 *cross section for the formation of the f - meson. (PEP 4/9)*

selection and $\pi\pi/\mu\mu$ separation, PEP4/9 obtains :

$$\Gamma_{f\to\gamma\gamma} = 3.2 \pm 0.1 \pm 0.4\,\text{keV}$$

with a Q^2 dependence as shown in Fig. 3.11 . In evaluating the radiative width, it has been assumed that $\gamma\gamma \to$ f proceeds solely via helicity $\lambda = \pm 2$. The π-angular distribution shown in Fig. 3.11 is consistent with this assumption.Equal amounts of $\lambda = \pm 2$ and =0 amplitudes would result in $\Gamma_{f\to\gamma\gamma} = 3.6 \pm 0.1 \pm 0.5\,\text{keV}$

.

Table 3.2 summarizes the currently available data on the radiative widths of the pseudoscalar and tensor mesons.

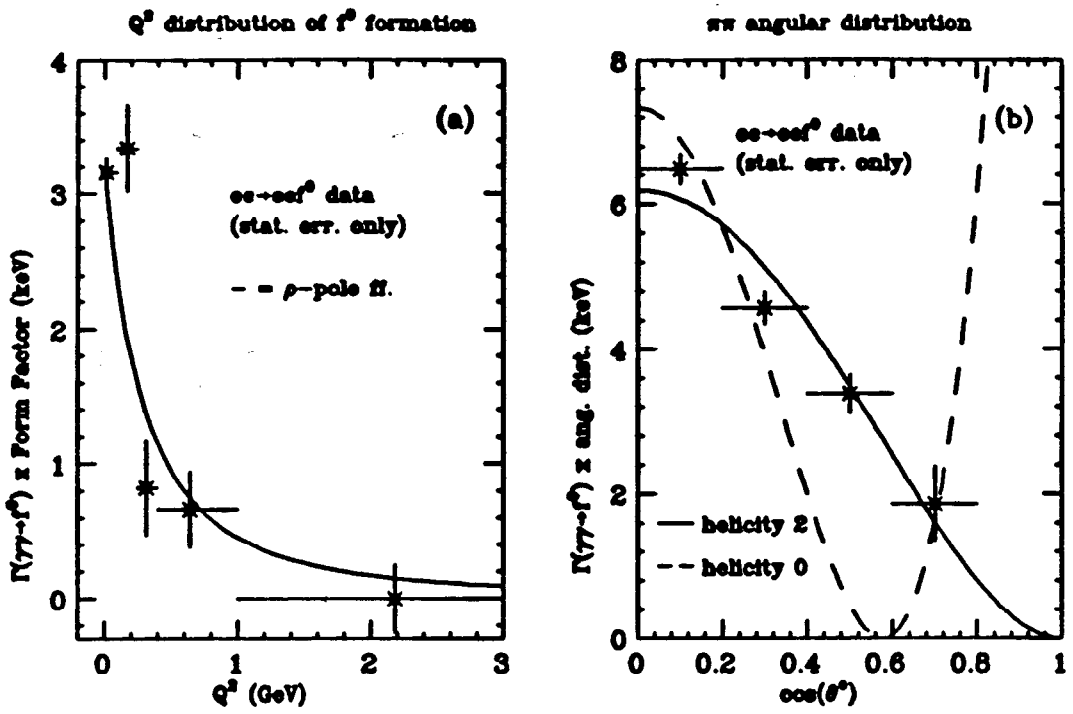

Fig. 3.11 *Q^2 dependence of the radiative width of the f - meson ; b. Angular distribution of the decay pion in f- decay .*

3.2 MIXING AND NONET SYMMETRY

The radiative widths of neutral, bare pseudoscalar and tensor mesons are related to their quark content by:

$$\Gamma_{X\to\gamma\gamma} \sim g^2 m_x^3 \tag{3.1}$$

where g is proportional to the net squared quark charge.

In the absence of gluonium the physical particles are related to the bare states by the well-known relations :

$$|\eta\rangle = F_8 \cos\theta|\eta_8\rangle - F_1 \sin\theta|\eta_1\rangle; \qquad |\eta'\rangle = F_8 \sin\theta|\eta_8\rangle + F_1 \cos\theta|\eta_1\rangle \tag{3.2}$$

For the physical mesons, this leads to relations involving the mixing angle θ and the ratio $r = F_1/F_8$ of the singlet and octet wave functions at the origin, or,

ATHERTON	PREPRINT	$\Gamma_{\pi^0\to\gamma\gamma} =$	$7.34 \pm 0.18 \pm 0.11 \times 10^3$
BEMPORAD*	PL 25B (1967) 380	$\Gamma_{\eta\to\gamma\gamma} =$	1.21 ± 0.26
BROWMAN*	PRL 32 (1974) 1067	"	0.324 ± 0.046
WEINSTEIN (CB)	PR D28 (1983) 2896	"	$0.56 \pm 0.12 \pm 0.09$
BARTEL (JADE)	DESY 85-033	"	$0.53 \pm 0.04 \pm 0.04$
AIHARA (PEP4/9)	-	"	$0.61 \pm 0.13 \pm 0.12$
BINNIE	PL 83B (1979) 141	$\Gamma_{\eta'\to\gamma\gamma} =$	5.4 ± 2.1
BARTEL (JADE)**	PL 113B (1982) 190	"	$5.0 \pm 0.5 \pm 0.9$
JENNI (MKII)**	PR D27 (1983) 1031	"	$5.8 \pm 1.1 \pm 1.2$
BEHREND (CELLO)**	PL 114B (1984) 378	"	$6.0 \pm 1.1 \pm 0.8$
BERGER (PLUTO)	PL 142B (1984) 125	"	$3.8 \pm 0.26 \pm 0.43$
ALTHOFF (TASSO)	PL 147B (1984) 487	"	$5.1 \pm 0.4 \pm 0.7$
AIHARA (PEP4/9)	-	"	$4.2 \pm 0.3 \pm 0.6$
EDWARDS (CB)	PL 110B (1982) 82	$\Gamma_{A_2\to\gamma\gamma} =$	$0.77 \pm 0.18 \pm 0.27$
BEHREND (CELLO)	PL 114B (1982) 378	"	$0.81 \pm 0.19 \pm 0.27$
BERGER (PLUTO)	PL 149B (1984) 427	"	$1.06 \pm 0.18 \pm 0.19$
ALTHOFF (TASSO)	PL 121B (1982) 216	$\Gamma_{f'\to\gamma\gamma} =$	$0.11 \pm 0.02 \pm 0.04$
BERGER (PLUTO)	PL 94B (1980) 254	$\Gamma_{f\to\gamma\gamma} =$	$2.3 \pm 0.5 \pm 0.35$
ROUSSARIE (MKII)	PL 105B (1981) 304	"	$3.6 \pm 0.3 \pm 0.5$
BRANDELIK(TASSO)	Z PHYS C10 (1981) 117	"	$3.2 \pm 0.2 \pm 0.6$
EDWARDS (CB)	PL 110B (1982) 82	"	$2.7 \pm 0.2 \pm 0.6$
BEHREND (CELLO)	Z PHYS C23 (1984) 223	"	$2.5 \pm 0.1 \pm 0.5$
SMITH (MKII)	PR D30 (1984) 851	"	$2.52 \pm 0.13 \pm 0.38$
BERGER (PLUTO)	Z PHYS C26 (1984) 199	"	$3.25 \pm 0.25 \pm 0.5$
COURAU (DELCO)	PL 174B (1984) 227	"	$2.70 \pm 0.05 \pm 0.2$
AIHARA (PEP4/9)	-	"	$3.2 \pm 0.1 \pm 0.4$

Table 3.2 *1985 Summary of the radiative widths (in keV) of the pseudoscalar and tensor mesons.* * *Measurement of the Primakoff effect.* ** *Data evaluated assuming the decay matrix to be constant.*

alternatively, to relations involving the fractional content of normal (u, d) and strange quarks. For pseudoscalars:

RESULTS ON NEUTRAL PSEUDOSCALAR AND TENSOR MESONS IN $\gamma\gamma \to M$	
PSEUDOSCALARS	**TENSORS**
$\Gamma_{\eta\to\gamma\gamma} = 0.54 \pm 0.05$	$\Gamma_{f'\to\gamma\gamma} = 0.11 \pm 0.05$
$\Gamma_{\eta'\to\gamma\gamma} = 4.21 \pm 0.35$	$\Gamma_{f\to\gamma\gamma} = 2.81 \pm 0.14$
$\Gamma_{\pi^0\to\gamma\gamma} = 7.34 \pm 0.21 \times 10^{-3}$	$\Gamma_{A_2\to\gamma\gamma} = 0.91 \pm 0.17$
$r_p = 0.94 \pm 0.04$	$r_t = 1.09 \pm 0.12$
$\theta = -19.0° \pm 1.8°$	$\theta = 26.6° \pm 2.6°$
θ (MASS FORMULA) $= \pm 11°$	$\pm 28°$
θ (IDEAL MIXING) $= 35.3°$	$35.3°$
quark η u,d = 64%	f' u,d = 71.3%
content " s = 36%	" s = 98.3%
η' u,d = 32%	f u,d = 96%
" s = 68%	" s = 4%
ratio $\left(\frac{\eta_1}{\eta_8}\right)^2_\eta$ = 10%	$\left(\frac{f_1}{f_8}\right)^2_{f'}$ = 30%
" $\left(\frac{\eta_8}{\eta_1}\right)^2_{\eta'}$ = 13%	$\left(\frac{f_8}{f_1}\right)^2_{f}$ = 21%

Table 3.3 *Mixing angles and quark content of the pseudoscalar and tensor mesons.*

$$\left(\frac{m_{\pi^0}}{m_\eta}\right)^3 \frac{\Gamma_{\eta\to\gamma\gamma}}{\Gamma_{\pi^0\to\gamma\gamma}} = \left(\frac{\cos\theta - 2\sqrt{2}r_p \sin\theta}{\sqrt{3}}\right)^2 = \frac{25}{9}|x_\eta + \frac{\sqrt{2}}{5}y_\eta|^2 \qquad (3.3)$$

and:

$$\left(\frac{m_{\pi^0}}{m_{\eta'}}\right)^3 \frac{\Gamma_{\eta'\to\gamma\gamma}}{\Gamma_{\pi^0\to\gamma\gamma}} = \left(\frac{\sin\theta + 2\sqrt{2}r_p \cos\theta}{\sqrt{3}}\right)^2 = \frac{25}{9}|x_{\eta'} + \frac{\sqrt{2}}{5}y_{\eta'}|^2 \qquad (3.4)$$

$$\text{with} \quad |\eta\rangle = x_\eta |(u\bar{u} + d\bar{d})/\sqrt{2}\rangle + y_\eta |s\bar{s}\rangle \quad \text{etc.} \qquad (3.5)$$

By adding (3.3) and (3.4) , a sum rule is obtained which is independent of θ.

For tensors the corresponding relations are obtained with the substitution $\eta \rightarrow f', \eta' \rightarrow f, \pi^0 \rightarrow A_2, r_p \rightarrow r_t$.

Using (3.2) to (3.4) with the weighted averages of all currently available results obtained in $\gamma\gamma$ collisions (table 3.2 ,July 1985 ,excluding "Primakoff" measurements of the η width ,and η' data analyzed with a constant matrix element in the Monte Carlo) one arrives at the results listed in table 3.3 . For both pseudoscalars and tensors the data are in agreement with the values $r_p = 1.0$, $r_t = 1.0$, expected on the basis of nonet symmetry. The pseudoscalar mixing angle is in disagreement with the angle obtained from the mass formula. For the tensors there is agreement to within one standard deviation. The quark contents (x^2, y^2) have been calculated assuming no contributions from heavy quarks or glue. The f' is almost pure s , while f is mostly u , d. The η consists for about 2/3 of normal quarks , for 1/3 of strange quarks. For η' the situation is the reverse. The η and η' are $\sim$ 90% pure η_8 , resp. η_1 states. Assuming exact nonet symmetry does not alter the conclusions on the quark content significantly.

3.3 GLUONIUM, ANYWHERE?

Figs. 3.12 and Fig. 3.13 show the x, y diagrams indicating the normal and strange quark content of the η, η' and f'/f mesons, as computed from the data in table 3.3 . The radiative widths of the $\gamma\gamma$ experiments determine a relation between x and y, as defined in (3.5) , and do not by themselves rule out contributions due to heavy quarks and gluonium. Rosner[14] has pointed out that limits on quarkonium –gluonium mixtures can be obtained from the overlap of the $\gamma\gamma$ decays discussed with other radiative decays which are also sensitive to the quark content of the mesons. From ref. 14 and the data available in the literature on $\omega \rightarrow \pi\gamma$, $\phi \rightarrow \eta\gamma$, $\rho \rightarrow \eta\gamma$ and $\eta' \rightarrow \rho\gamma$ we obtain the bands parallel to the x and y axes in Fig.3.12 .

In Fig. 3.12 ,the shaded regions indicate the (one standard deviation) overlap

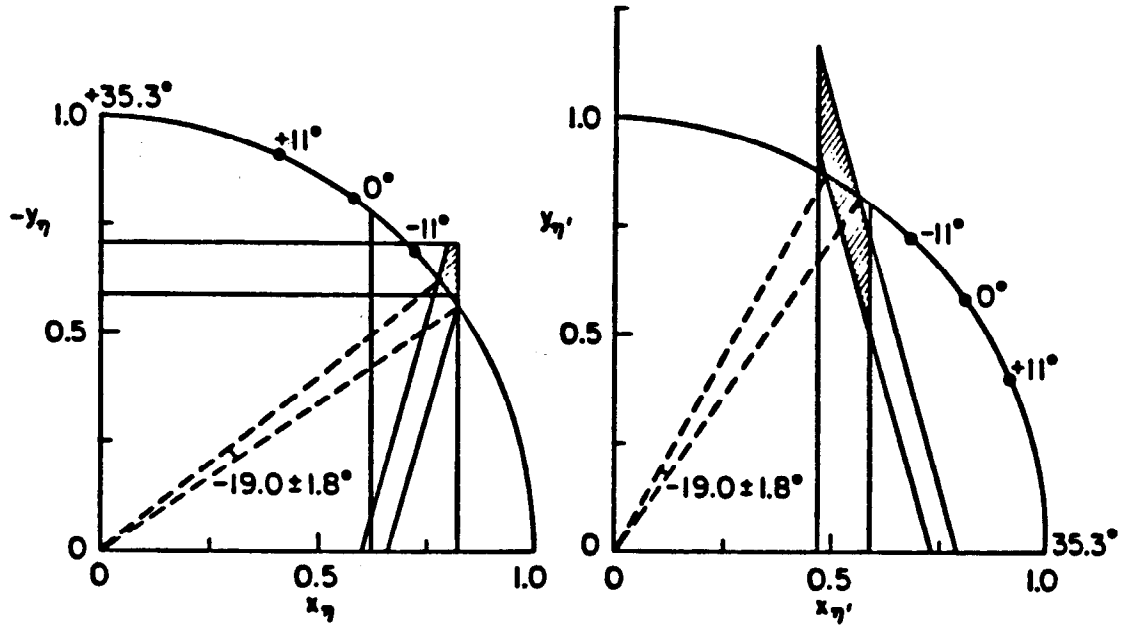

Fig. 3.12 *The normal (x^2) and strange (y^2) quark content of the η (a) and η' (b) mesons based on the data in table 3.3*

between the different measurements.The intersection with the circle indicates the range of x and y in the absence of gluonium. From the center of gravity of the region of overlap we obtain for the gluonium content $z^2 = 1 - x^2 - y^2$ for the η and the η' :

$$z^2(\eta) = -0.07 \pm 0.09$$

$$z^2(\eta') = +0.06 \pm 0.36$$

The conclusion is therefore that the upper limit for gluonium in the η is $\sim$ 10%(95% CL) while in the η' the upper limit is $\sim$ 40% at a confidence level of 70%, and leaves room for a substantial fraction of gluonium.

For the tensor mesons it is evident from Fig. 3.13 that the f(1270) is a mostly normal resonance ,with no room for gluonium . The f' ,on the other

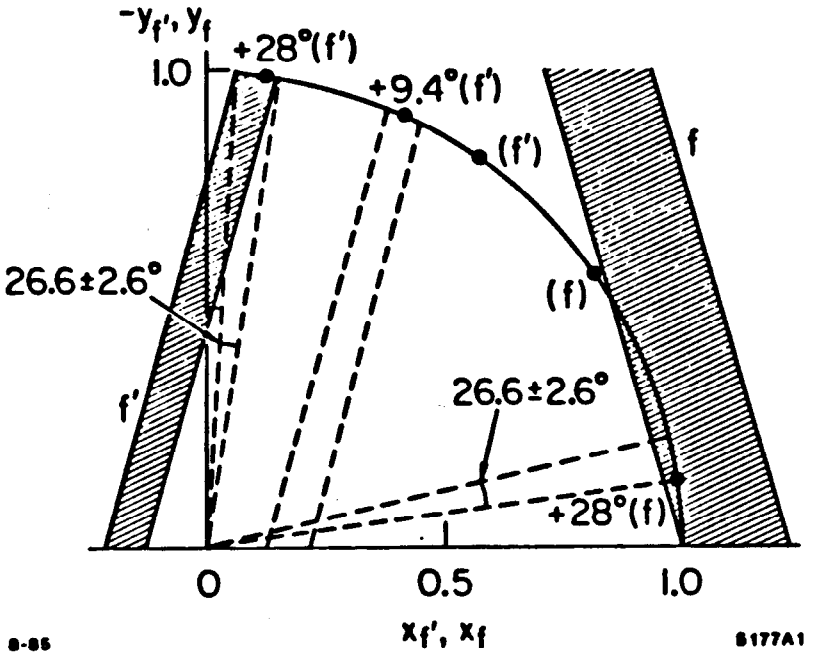

Fig. 3.13 *The normal(x^2) and the strange (y^2) quark content of the f' and the f meson ,based on the data in table 3.3 .The skew dashed band indicates a second solution,incompatible with the* f' → KK *branching ratio .*

hand , could be a mixture of strange quarks and gluonium , in a ratio which can not be obtained from a more accurate measurement of its radiative width alone. Clearly , setting good limits on $\gamma\gamma \rightarrow \iota$ and $\gamma\gamma \rightarrow \theta$ are the next step in the search for gluonium .

I am indebted to W.G.J.Langeveld for discussions and to E. Sullivan for taking excellent care of the manuscript.I would like to thank L.Montanet and collaborators for organizing a most pleasant conference at Autun .

REFERENCES

1) H. Euler and B. Kockel, *Nat. Wiss.* **23** (1935), 246.

2) G. Breit and J.A. Wheeler, *Phys. Rev.* **46** (1934), 1087.

3) S.J. Brodsky and G.P. Lepage, *Phys. Rev. D* **24** (1981), 1808).

4) W.G.J. Langeveld, Ph.D. Thesis, University of Utrecht, the Netherlands, 1985.

5) G. Gidal, paper presented at *the XVIth Symposium on Multi-particle Dynamics , 9 - 14 June 1985 ,Kiryat - Anavim ,Israel*

6) N.N. Achasov et al., *Z. Phys.* **C16** (1982), 55.

7) B.A. Li and K.F. Liu, *Phys. Rev.* **D30** (1984), 613.

8) M. Althoff et al., *Phys. Lett.* **130B** (1983), 449.

9) G.R. Farrar et al., Rutgers University, RU-85-08.

10) P.H. Damgaard, *Nucl. Phys.* **B211** (1983), 435.

11) M. Althoff et al., *Phys. Lett.* **142B** (1984), 135.

12) W. Bartel et al., DESY 85-033, April 1985.

13) Chr.Berger et al., *Phys. Lett.* **142B** (1984),125.

14) J. Rosner, *Phys. Rev.* **D27** (1983), 1101.